Wide Spectral Range Nonlinear Optical Crystals of One-Dimensional Coordination Solids $[Et_4N][Cd(SCN)_3]$ and $[Et_4N][Cd(SeCN)_3]$ and the General Design Criteria for $[R_4N][Cd(XCN)_3]$ (Where R = Alkyl and X = S, Se, Te) as NLO Crystals

Hong Zhang,*,† David E. Zelmon,† Gary E. Price,‡ and Boon K. Teo*,§

Materials Directorate, Air Force Research Laboratory (AFRL/MLPO), Wright-Patterson AFB, Ohio 45433-7707, University of Dayton Research Institute, 300 College Park Drive, Dayton, Ohio 45469, and Department of Chemistry, University of Illinois at Chicago, 845 West Taylor Street, Chicago, Illinois 60607

Received November 2, 1999

We report herein two new nonlinear optical (NLO) crystals, $[Et_4N][Cd(XCN)_3]$, where X = S (**1**) and Se (**2**), that are transparent from 220 to 3300 nm, covering the entire near-ultraviolet, the visible, and the near-infrared spectral regions and giving rise to a very wide and continuous optical window, which is useful for many frequency conversion applications. Both **1** and **2** exhibit highly efficient second harmonic generation (SHG) as measured via the Kurtz−Perry method. The corresponding $[Me_4N]^+$ salts, $[Me_4N][Cd(XCN)_3$ where X = S (**3**) and Se (**4**), show no SHG effects. All four structures adopt noncentrosymmetric space groups ($Cmc2_1$ for **1** and **2** and $Pna2_1$ for **3** and presumably **4**) and are based on one-dimensional anionic $[Cd(XCN)_3^-]_\infty$ zigzag chains. However, a detailed analysis of the structures of $[R_4N][Cd(XCN)_3]$, where R = Et, Me, and X = S, Se revealed that the difference in the second-order nonlinear responses of the Et_4N^+ salts (**1** and **2**) and the Me_4N^+ salts (**3** and **4**) is attributable to the relative alignment of the $[Cd(XCN)_3^-]_\infty$ zigzag chains, being parallel in the crystals of **1** and **2** but antiparallel in the crystals of **3** and **4**. Also reported, for the first time, are the synthesis and crystal structure of $[Et_4N][Cd(SeCN)_3]$ (**2**). Compound **2** crystallizes in an orthorhombic unit cell of $Cmc2_1$ space group symmetry with lattice parameters of 9.938(1) Å, 16.868(2) Å, 11.054(1) Å, and $Z = 4$. Other issues related to the molecular and crystal engineering of this class of NLO materials are also discussed.

I. Introduction

Nonlinear optical crystals play an important role in the development of photonics technology. Photonics is the analogue of electronics in which photons, instead of electrons, are used in the acquisition, storage, transmission, and processing of information.[1] In photonics, a growing need continues for low cost, high nonlinearity, efficient and high-quality crystals for birefringent phase-matchable optical parametric oscillators (OPO), optical parametric amplifier operation, and second-harmonics generation (SHG). The applications of nonlinear crystals that show such desirable properties as SHG and OPO (e.g., silver gallium selenide, zinc germanium phosphide, thallium arsenic selenide, etc.) are often limited by the spectral range as well as such factors as the quality, the cost of growth, and the ease of engineering of the crystals.[2−4] We report herein two nonlinear optical (NLO) crystals, $[Et_4N][Cd(XCN)_3]$, where X = S (**1**) and Se (**2**), which are transparent from 220 to 3300 nm, covering the entire near-ultraviolet, visible, and near-infrared spectral regions. Such a wide frequency range of transparency is of prime importance in frequency doubling (SHG) and other device applications.

The discovery of **1** and **2** as new NLO materials, reported here for the first time, is an outgrowth of our recent study of a series of NLO crystals,[5−8] based on polymeric cadmium−thiocyanate anions[9−13] and crown-ether−metal cations.[14−17] This new series of coordination solids may be described as inorganic

† Wright-Patterson AFB.
‡ University of Dayton Research Institute.
§ University of Illinois at Chicago.

(1) Prasad, P. N.; Williams, D. J. *Introduction to Nonlinear Optical Effects in Molecular and Polymers*; Wiley-Interscience: New York, 1991.
(2) Dmitriev, V. G.; Gurzadayan, G. G.; Nikogosyan, D. N. *Handbook of Nonlinear Optical Crystals*; Springer-Verlag: New York, 1991.
(3) (a) Jackson, A. G.; Ohmer, M. C.; LeClair, S. R. *Infrared Phys. Technol.* **1997**, *38*, 233. (b) Fischer, D. W.; Ohmer, M. C.; McCrae, J. E. *J. Appl. Phys.* **1997**, *81*, 3579.
(4) Singh, N. B.; Henningsen, T.; Balakrishna, V.; Suhre, D. R.; Fernelius, N.; Hopkins, F. K.; Zelmon, D. E. *J. Cryst. Growth* **1996**, *161*, 398.
(5) Zhang, H.; Wang, X.; Teo, B. K. *J. Am. Chem. Soc.* **1996**, *118*, 11813.
(6) (a) Zhang, H.; Wang, X.; Zhu, H.; Xiao, W.; Teo, B. K. *J. Am. Chem. Soc.* **1997**, *119*, 5463. (b) Zhang, H.; Wang, X.; Zhu, H.; Xiao, W.; Teo, B. K. *Inorg. Chem.* **1999**, *38*, 886.
(7) Zhang, H.; Wang, X.; Zhang, K.; Teo, B. K. *Inorg. Chem.* **1998**, *37*, 3490.
(8) Zhang, H.; Wang, X.; Zhang, K.; Teo, B. K. *Coord. Chem. Rev.* **1999**, *183*, 157.
(9) (a) *Chemistry and Biochemistry of Thiocyanic Acid and Its Derivatives*; Newman, A. A., Ed.; Academic Press: New York, 1975. (b) *Chemistry of Pseudohalides*; Golub, A. M., Kohler, H., Skopenko, V. V., Eds.; Elsevier: Amsterdam, 1986.
(10) (a) Basolo, F. *Coord. Chem. Rev.* **1968**, *3*, 213. (b) Burmeister, J. L. *Coord. Chem. Rev.* **1968**, *3*, 225.
(11) (a) Kuniyasu, Y.; Suzuki, Y.; Taniguchi, M.; Ouchi, A. *Bull. Chem. Soc. Jpn.* **1987**, *60*, 179. (b) Taniguchi, M.; Ouchi, A. *Bull. Chem. Soc. Jpn.* **1989**, *62*, 424−428.
(12) (a) Thiele, V. G.; Messer, D. *Z. Anorg. Allg. Chem.* **1980**, *646*, 255. (b) Gronbaek, R.; Dunitz, J. D. *Helv. Chim. Acta* **1964**, *47*, 1889−1897.
(13) Eichele, K.; Wasylishen, R. E. *Inorg. Chem.* **1994**, *33*, 2766.
(14) Pedersen, C. J. *J. Am. Chem. Soc.* **1967**, *89*, 2495.
(15) Lehn, J. M. *Acc. Chem. Res.* **1978**, *11*, 49.
(16) (a) Cram, D. J.; Cram, J. M. *Acc. Chem. Res.* **1978**, *11*, 8 and references therein. (b) Stoddart, J. F. *Chem. Soc. Rev.* **1979**, *8*, 85 and references therein.

10.1021/ic9912833 CCC: $19.00
Published on Web 04/12/2000

polymers with organic spacers (IPOS), a class of hybrid materials combining the advantageous properties of inorganic, organic, and polymeric materials.[18−21] Indeed, the title compounds $[R_4N][Cd(XCN)_3]$, where R = Et, X = S (**1**), Se (**2**); R = Me, X = S (**3**), Se (**4**), are members of the IPOS series, which have been predicted by us to be potential NLO crystals because of the tetrahedral shape of the tetraalkylammonium cations.

Specifically, on the basis of our previous systematic synthetic and structural studies,[5−8] it was found that in these coordination solids, the anionic cadmium−thiocyanate polymers can form a wide variety of structures ranging from one-dimensional (1-D) single-chain structures[5,7,8] to two-dimensional (2-D) layered structures.[6] The arrangement and the alignment of these anionic cadmium−thiocyanate chains can be controlled by the cations. In particular, it was reasoned that tetrahedrally coordinated tetraalkylammonium cations, which lack inversion symmetry, should induce formation of noncentrosymmetric space groups, making them potential second-order nonlinear optical crystals.

We report here the NLO properties (in terms of SHG) of $[Et_4N][Cd(SCN)_3]$ (**1**)[11a] and $[Et_4N][Cd(SeCN)_3]$ (**2**). The synthesis and crystal structure of **2** are also reported here for the first time. The tetramethylammonium analogues of **1** and **2**, namely, $[Me_4N][Cd(SCN)_3]$ (**3**) and $[Me_4N][Cd(SeCN)_3]$ (**4**), are also included in our NLO study. Much to our initial surprise, while all these structures are based on one-dimensional anionic $[Cd(XCN)_3^-]_\infty$ zigzag chains and crystallize in noncentrosymmetric space groups, only the tetraethylammonium salts (**1** and **2**) give rise to efficient SHG effects. Both **3** and **4**, the corresponding tetramethylammonium salts, were found to exhibit no SHG effect. A detailed analysis of the structures of $[R_4N][Cd(XCN)_3]$, where R = Et, X = S (**1**), Se (**2**); R = Me, X = S (**3**), Se (**4**), revealed that the difference in the second-order NLO properties is due to the fact that the relative alignment of the $[Cd(XCN)_3^-]_\infty$ zigzag chains in the Et_4N^+ salts (**1** and **2**) is parallel, whereas the corresponding arrangement in the Me_4N^+ salts (**3** and **4**) is antiparallel. Other issues related to the molecular and crystal engineering of this class of NLO materials and their potential applications in wide spectral range frequency conversion of coherent laser light will also be addressed. Finally, it should be emphasized that high-quality, large (centimeter-sized) single crystals of these coordination solids can be grown from aqueous solutions, making them candidates for technological applications.

(17) (a) Dobler, M.; Dunitz, J. D.; Seiler, P. *Acta Crystallogr.* **1974**, *B30*, 2741. (b) Bush, M. A.; Truter, M. R. *J. Chem. Soc., Perkin Trans.* **1972**, *2*, 345. (c) Dobler, M.; Phizackerley, R. P. *Acta Crystallogr.* **1974**, *B30*, 2748. (d) Hughes, D. L. *J. Chem. Soc., Dalton Trans.* **1975**, 2374.

(18) (a) Khodia, S.; Josse, D.; Zyss, J. *J. Opt. Soc. Am. B* **1998**, *15*, 751. (b) Kotler, Z.; Hierle, R.; Josse, D.; Zyss, J.; Masse, R. *J. Opt. Soc. Am. B* **1992**, *9*, 534.

(19) Rosker, M.; Cunningham, P.; Ewbank, M. D.; Marcy, H. O.; Vachss, F. R.; Warren, L. F.; Gappinger, R.; Borwick, R. *Pure Appl. Opt.* **1996**, *5*, 667.

(20) (a) Desiraju, G. R. *Crystal Engineering*; Elsevier: Amsterdam,1989; Chapter 8. (b) Wright, J. D. *Molecular Crystals*, 2nd ed.; Cambridge University Press: New York, 1995. (c) *Structure and Properties of Molecular Crystals*; Pierrot, M., Ed.; Elsevier: Amsterdam, 1990.

(21) (a) Stucky, G. D.; MacDougall, J. E. *Science* **1990**, *247*, 669. (b) Meyer, F.; Bredas, J. L.; Zyss, J. *J. Am. Chem. Soc.* **1992**, *114*, 2914. (c) Schwiebert, K. E.; Chin, D. N.; MacDonald, J. C.; Whitesides, G. M. *J. Am. Chem. Soc.* **1996**, *118*, 4018. (d) Philp, D.; Stoddart, J. F. *Angew. Chem., Int. Ed. Engl.* **1996**, *35*, 1154. (e) Thalladi, V. R.; Brasselet, S.; Weiss, H.; Blaser, D.; Katz, A. K.; Carrell, H. L.; Boese, R.; Zyss, J.; Nangia, A.; Desiraju, G. R. *J. Am. Chem. Soc.* **1998**, *120*, 2563.

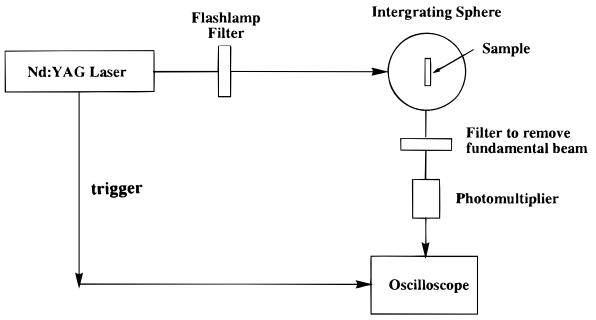

Figure 1. Powder measurement setup of second-order nonlinear optical effects.

II. Experiments

Preparations and Characterization. All reagents were purchased from Aldrich Chemicals and were used without further purification. Compounds **1** and **3** were prepared according to the literature method.[11] Compounds **2** and **4** were prepared as follows. With vigorous stirring, 20 mL of an aqueous solution of 1 M Et_4NCl (for **2**) or 20 mL of an aqueous solution of 1 M Me_4NCl (for **4**) was added dropwise to a preformed mixture of 50 mL of 0.35 M aqueous solution of $CdSO_4$ and 50 mL of 1 M aqueous solution of KSeCN, respectively, over a period of 30 min. The solution mixture was then cooled with an ice bath. Fine crystals that formed after 2 days were collected by filtration and dried in a vacuum oven. Elemental analyses gave satisfactory results for all compounds. The analytical results for the new compounds, **2** and **4**, are as follows. Anal. Calcd (found) for $[Et_4N][Cd(SeCN)_3]$ (**2**) (fw = 557.60): C, 23.69 (23.86); H, 3.61 (3.31); N, 10.05 (10.14); Se, 42.5 (40.6); Cd, 20.2 (20.2). Anal. Calcd (found) for $[Me_4N][Cd(SeCN)_3]$ (**4**) (fw = 501.6): C, 16.75 (16.64); H, 2.39 (2.33); N, 11.16 (11.29); Se, 47.2 (46.1); Cd, 22.4 (22.7). The UV−vis−NIR spectra, measured with a CARY 5E spectrophotometer, show a wide spectral range of transparency from 220 to 3000 nm for compounds **1**−**4**. The first electronic absorption band, which is believed to be due to the metal-to-ligand charge transfer (MLCT) (or metal-mediated ligand $\pi \rightarrow \pi^*$ transition), occurs at 220 nm (with a slight shoulder at 262 nm). The first IR absorption bands, as recorded by a BIO-RAD FTS-40 spectrophotometer, occur at around 3333 nm (2900−3000 cm^{-1}). The mid- and far-IR regions exhibit the functional groups of both the cation and the anion. In particular, the ν(C−N) peaks of the bridging SCN^- ligands at 2100 cm^{-1} and $SeCN^-$ ligands at 2111 cm^{-1} are indicative of the $[Cd(SCN)_3^-]_\infty$ and $[Cd(SeCN)_3^-]_\infty$ chains, respectively.[5−8]

Nonlinear Optical Property Measurements. The title compounds were examined for their nonlinear optical properties using the Kurtz−Perry powder method.[22] The experimental setup is shown in Figure 1. The crystalline compounds were ground into powders and graded using standard sieves into sizes ranging from 3 to 300 μm and packed into spectrometer cells each having a 1 mm path length. The cell was then placed at the center of an integrating sphere. The output from a Nd:YAG laser operating at 1.064 μm was attenuated and allowed to impinge on the sample. Pulse energy was 150 mJ into the attenuator, and the repetition rate was 70 Hz. A filter was placed in front of the integrating sphere to eliminate any stray visible light. A Hamamatsu R1463 photomultiplier tube with a range 185−850 nm was used to detect the 0.532 μm second harmonic radiation generated by the powder samples. An additional optical filter was used at the front end of the photomultiplier tube to ensure that there was no response due to 1.064 μm radiation entering the integrating sphere. The output from the photomultiplier tube was recorded with Keithley 195 digital multimeter and a Gould model 4074 digital storage oscilloscope.

The spectral content of the output signals from the title compounds **1** and **2** was analyzed with a monochromator and the photomultiplier assembly described above. Here, the average particle size was 150 μm. Once again, the input beam was the 1.064 μm radiation from the Nd:YAG laser. The pulse energy used was 20 mJ for **1** and KH_2PO_4 (KDP) and 3 mJ for **2** (due to the lower radiation damage threshold of the

(22) Kurtz, S. K.; Perry, T. T. *J. Appl. Phys.* **1968**, *39*, 3798.

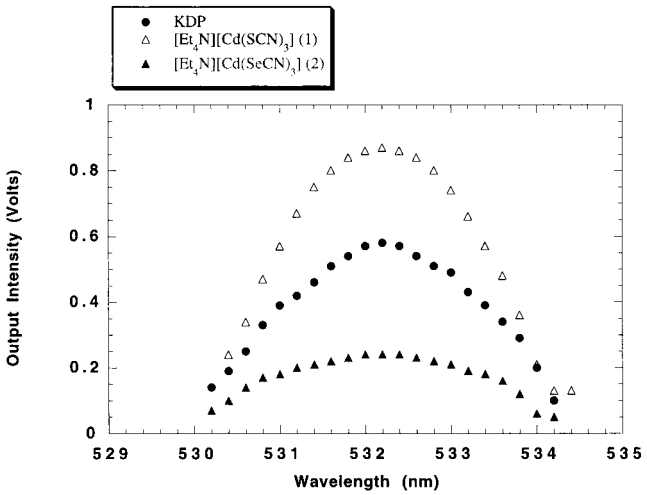

Figure 2. Spectral content of the second harmonic generation signals for 1.064 μm Nd:YAG laser. Note that KH_2PO_4 (KDP) and $[Et_4N][Cd(SCN)_3]$ (**1**) were both measured using 20 mJ per pulse of input laser beam whereas the input beam was attenuated to approximately 3 mJ per pulse for the measurement of $[Et_4N][Cd(SeCN)_3]$ (**2**).

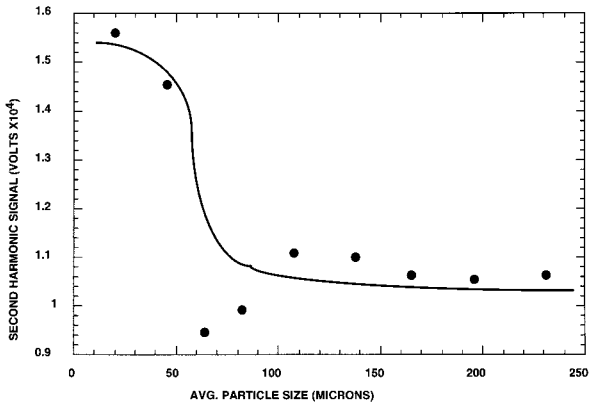

Figure 3. Intensity of second harmonic signal versus particle size for $[Et_4N^+][Cd(SCN)_3^-]$ (**1**).

latter). The green light output was collected by an optical fiber bundle that was coupled to a CVI 240 $^1/_4$ m monochromator. The monochromator was scanned from 525 to 540 nm, and the intensity of the monochromatized beam was measured as a function of wavelength. The results are compared with the results of KDP in Figure 2. Each data point in Figure 2 represents an average of 25 readings of the output light intensity, which have standard deviations of less than 1% for all particle sizes. It can be seen from Figure 2 that the spectral content of the output beams from **1**, **2**, and KDP is virtually identical and centered at 532.2 nm. Qaulitatively, for the powder size of 150 μm **1** and **2** are 1.5 and 3 times more efficient than KDP as SHG crystals, as judged by the intensity at 532 nm of the second harmonic radiation. However, these comparisons should be treated with extreme caution because they are highly dependent on the size and uniformity of the particles, as well as on the wavelength and power of the input laser light, etc.

The intensity of the second harmonic output signal (green light at 532 nm generated by the input beam at 1.064 μm) from the powder samples described above was also measured as a function of particle size. The results are plotted in Figures 3 and 4 for **1** and **2**, respectively. It should be pointed out that each data point (the *ordinate*) in these plots is the average of 25 readings of the output light intensities of each particle size. Furthermore, each particle size (the abscissa) represents the "average" particle size estimated from the upper and lower bounds of the successive sieves. The complete listings of the measured data for **1** and **2**, along with the standard deviations, can be found in Tables S1 and S2, respectively (Supporting Information). It can be seen from Figure 3 that the output light intensity from the powder samples of **1** peaks at approximately 20 μm and falls off significantly

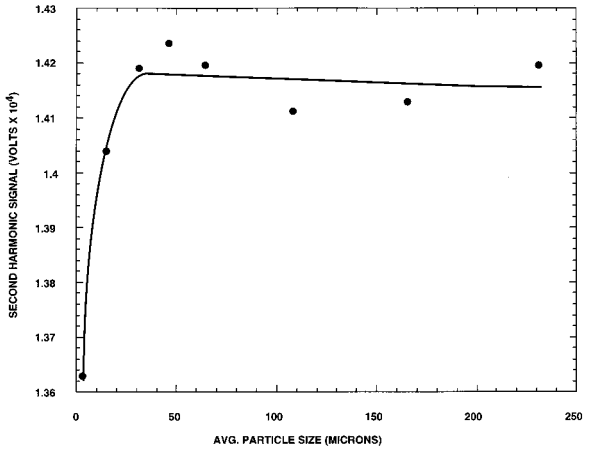

Figure 4. Intensity of second harmonic signal versus particle size for $[Et_4N^+][Cd(SeCN)_3^-]$ (**2**).

Table 1. Crystallographic Data for $[Et_4N][Cd(SeCN)_3]$ (**2**)

chemical formula	$CdSe_3N_4C_{11}H_{20}$
fw	557.60
space group	$Cmc2_1$
a (Å)	9.938(1)
b (Å)	16.868(2)
c (Å)	11.054(1)
V (Å^3)	1853.4(2)
Z	4
temp (°C)	25
λ (Å)	0.7109
ρ_{calcd} (g cm^{-3})	1.998
μ (cm^{-1})	70.663
R [a]	0.048
R_w [b]	0.063

[a] $R = \sum||F_o| - |F_c||/\sum|F_o|$. [b] $R_w = [\sum(w(|F_o| - |F_c|)^2)/\sum(wF_o^2)]^{1/2}$.

as the average particle size increases beyond 60 μm. The results for **2** are distinctly different, however. As is apparent from Figure 4, the green light output from the powder samples of **2** increases with the average particle size and reaches a plateau at 50−60 μm. This difference in the particle size dependence of the second harmonic light intensity points to the difference in phase matchability of the crystals of **1** and **2**. As will be discussed in detail later, these plots strongly suggest that **2** is phase-matchable while **1** is not.

X-ray Crystallography. The structures of compounds **1** and **3** have been reported in the literature.[11] Since the elemental analysis gave results consistent with the predicted formula, it was expected that compounds **2** and **4** would have the same structures as compounds **1** and **3**, respectively, with the selenium atoms substituting for the sulfur atoms. This was confirmed by the single-crystal X-ray structural analysis of compound **2**, which is isomorphous with **1**.

A colorless needle shape crystal of **2**, with dimensions of 0.12 mm × 0.09 mm × 0.20 mm, was selected and mounted on a glass fiber with epoxy resin. Room temperature (23 ± 2 °C) single-crystal X-ray diffraction data were collected on a Nonius CAD4 diffractometer using graphite-monochromatized Mo Kα radiation (λ = 0.710 69 Å). The observed intensities were corrected for Lorentz and polarization effects. A Wilson plot of the data favored noncentrosymmetric space groups. The space group of $Cmc2_1$ was uniquely defined by the systematic absences, which was later confirmed by the successful solution and refinement of the structure. Structural solution and refinements was performed using teXsan package of the Molecular Structural Corporation. Positions of the cadmium atoms and $SeCN^-$ ligands were determined by direct methods, and other nonhydrogen atoms were located via Fourier syntheses. Details of the crystallographic data are summarized in Table 1. Selected bond distances and angles are listed in Table 2. Complete crystallographic and structural details of **2** are provided in the Supporting Information.

Table 2. Selected Bond Lengths (Å) and Angles (deg) for $[Et_4N][Cd(SeCN)_3]$ (**2**)

Cd1−Se1	2.850(3)	Se1−C1	1.74(2)
Cd1−Se2	2.794(2)	Se2−C2	1.88(2)
Cd1−N1	2.33(2)	N1−C1	1.14(3)
Cd1−N2	2.37(2)	N2−C2	1.10(2)
Se1−Cd1−Se2	86.96(6)	N2−Cd1−N2	79.5(8)
Se1−Cd1−N1	177.1(5)	Cd1−Se1−C1	93.7(7)
Se1−Cd1−N2	90.1(3)	Cd1−Se2−C2	95.8(5)
Se2−Cd1−Se2	101.04(10)	Cd1−N1−C1	161(1)
Se2−Cd1−N1	91.2(3)	Cd1−N2−C2	148(1)
Se2−Cd1−N2	168.7(4)	Se1−C1−N1	178(2)
Se2−Cd1−N2	89.7(4)	Se2−C2−N2	176(1)
N1−Cd1−N2	92.1(5)		

III. Results

Syntheses. The title compounds were prepared according to the reaction

$$R_4NCl + 3KXCN + CdSO_4 \xrightarrow{H_2O} [R_4N][Cd(XCN)_3] + K_2SO_4 + KCl$$

where R = Et, X = S (**1**), Se (**2**); R = Me, X = S (**3**), Se (**4**). Preparative details are given in the experimental section for the two new compounds, **2** and **4**, only.

The chalcogenocyanate ions, XCN^-, where X = S, Se, or Te, are linear pseudohalides. They are highly versatile ambidentate ligands with two donor atoms that can coordinate to metals through either the nitrogen or the chalcogen (X) atoms, or both.[9−13] In fact, there are many modes of coordination of the XCN^- ligand to metals that may be either terminal or bridging. Combinations of various coordination modes give rise to a wide variety of metal chalcogenocyanate structures.[8]

The modes of metal coordination of chalcogenocyanate are best understood in terms of Pearson's hard−soft acid−base concept.[23] The X atom of the XCN^- (X = S (as in **1** and **3**), Se (as in **2** and **4**)) ligands, being a soft base, preferentially coordinates to the Cd(II) ion (with a d^{10} configuration), which may be considered as a soft acid. With appropriate stoichiometry, the ambidentate nature of the XCN^- ligand allows the formation of bridges between cadmium atoms as exemplified by the formation of the anionic infinite chain $[Cd(XCN)_3^-]_\infty$ in the title compounds **1**−**4**.

Nonlinear Optical Properties. Compounds **1** and **2** both showed strong second harmonic generation using 1.064 μm laser pump. The relative intensities of the second harmonic signal versus average particle size for compounds **1** and **2** are shown in Figures 3 and 4, respectively. These data indicate that second harmonic generation is achievable in both compounds **1** and **2**. Furthermore, compound **2** is birefringently phase-matchable for the 1.064 μm frequency-doubling process. For **1**, the second harmonic signal decreases significantly with increasing particle size, indicating that it is not phase-matchable for this nonlinear optical process. It was further observed that **2** has a lower radiation damage threshold than **1**. It was necessary to attenuate the input beam to approximately 3 mJ per pulse during the experiment. On the other hand, **1** was unaffected by pulse energies up to 20 mJ. In contrast, compounds **3** and **4** produced no second harmonic generation. These differences in the NLO responses can be rationalized by the important variations in their crystal structures, as we shall discuss next.

Crystal Structure of 2. Compound **2** crystallizes in an orthorhombic unit cell of dimensions of 9.938(1) Å, 16.868(2) Å, 11.054(1) Å, and space group $Cmc2_1$, with four $[Et_4N][Cd(SeCN)_3]$ per unit cell ($Z = 4$). Figures 5 and 6 depict the structure and crystal packing, respectively, of **2**, which is reported here for the first time. Note that Cd1, Se1, C1, and N1 reside on a crystallographic mirror plane (at $x = 0$) while the other two SeCN ligands (Se2−C2−N2) are related by the same mirror. We should point out that the Et_4N^+ cation, which is located at the mirror plane at $x = {}^1/_2$, is crystallographically disordered (50:50). Only one set of the disordered cations is shown in Figures 5 and 6b. It is interesting to note, however, that only the α carbons are 50:50 disordered; the β carbons (C32, C42, C122, and C122*), as well as the nitrogen atom (N3), of the Et_4N^+ cation are perfectly ordered. Furthermore, N3, C32, and C42 reside on the crystallographic mirror plane at $x = {}^1/_2$, whereas the remaining two β carbons (C122, and C122*) are related by the same mirror.

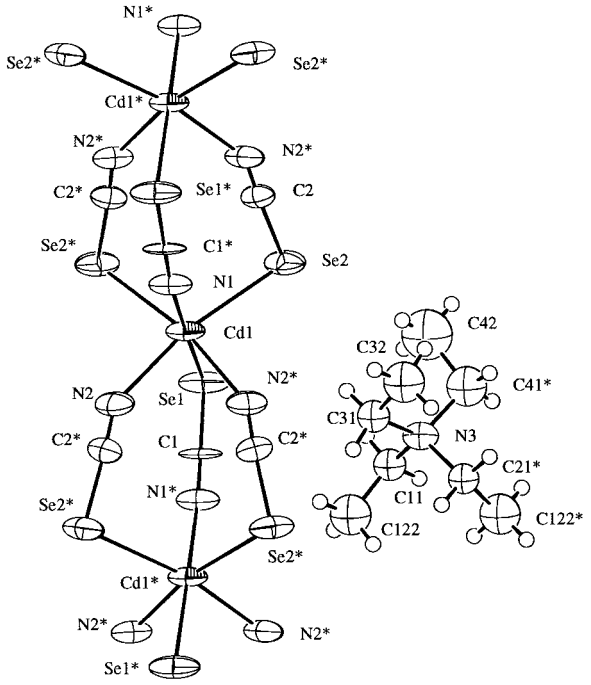

Figure 5. ORTEP diagram of $[Et_4N^+][Cd(SeCN)_3^-]$ (**2**) (50% thermal ellipsoids). We should point out that the Et_4N^+ cation is crystallographically disordered (50:50). Only one set of the disordered cation is shown (see text).

As observed in all of the title compounds, the Cd atoms in the infinite chains are octahedrally coordinated with three Se and three N atoms (in fac configuration) with N atoms trans to the Se atoms as a result of trans influence. Adjacent Cd atoms are linked by three bridging $SeCN^-$ ligands, forming infinite $[Cd(SeCN)_3^-]_\infty$ zigzag polymeric chains. The distance between Cd atoms (Cd···Cd) is 5.41 Å (av). The Cd···Cd···Cd angle is around 162° (av). The average Se−C and C−N distances of 1.83 and 1.11 Å, respectively, in **2**, indicate partial π delocalization for all three $(SeCN)^-$ chains winding around the central zigzag Cd_∞ chains. The average Se−C distance in **2** is 0.18 Å longer than the average S−C distance of 1.65 Å in the sulfur analogue (**1**), consistent with the fact that the atomic radius of Se is larger than that of S.

Pattern of Crystallization. As summarized in Table 3, all four title compounds crystallize in noncentrosymmetric space groups in the orthorhombic crystal system. With relatively large cations such as $(Et_4N)^+$, crystals **1** and **2** adopt the space group $Cmc2_1$, whereas with relatively small cations such as $(Me_4N)^+$, **3** and **4** adopt the space group $Pna2_1$. In both crystal types, the $[Cd(XCN)_3^-]_\infty$ zigzag chains are arranged in an approximate

(23) Pearson, G. S. *Adv. Inorg. Chem. Radiochem.* **1966**, *8*, 177.

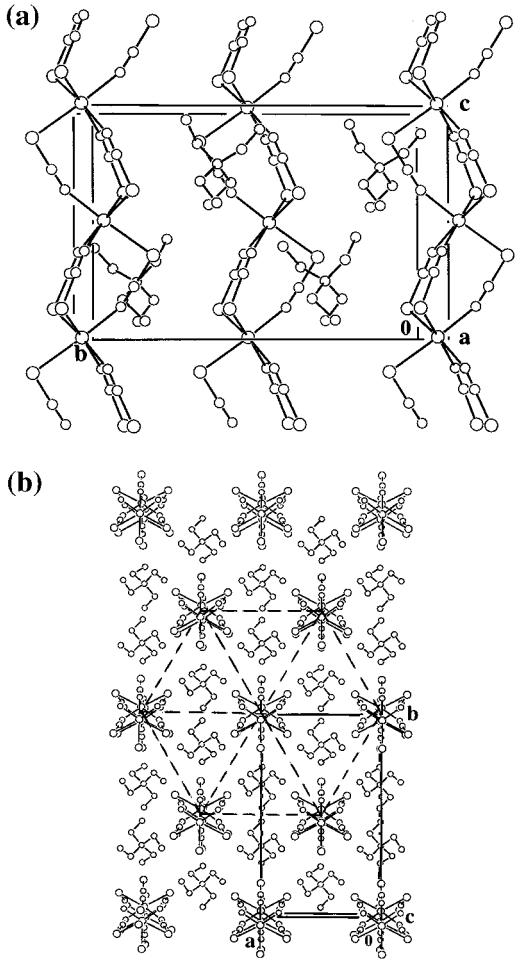

Figure 6. Crystal packing of $[Et_4N^+][Cd(SeCN)_3^-]$ (**2**) as viewed along (a) the crystallographic *a* axis and (b) the crystallographic *c* axis. Note that only one set of the disordered Et_4N^+ cation is shown (see text). As shown in (a), the $[Cd(SeCN)_3^-]_\infty$ zigzag chains are aligned parallel to one another and run along the crystallographic *c* axis. As shown in (b), the$[Cd(SeCN)_3^-]_\infty$ chains are arranged in an approximately hexagonal array with the $[Et_4N^+]$ cations occupying the triangular channels.

hexagonal array with the cations occupying the triangular channels (e.g., Figure 6b for **2**). The relative alignment of the anionic $[Cd(XCN)_3^-]_\infty$ zigzag chains, however, is strongly influenced by the size of the cations. With the larger $(Et_4N)^+$ cations, crystals **1** and **2** adopt a parallel alignment (Figure 7a) of the anionic $[Cd(XCN)_3^-]_\infty$ zigzag chains (see also Figure 6a for **2**), which are related by crystallographic *C*-centering in space group $Cmc2_1$, whereas with the relatively smaller $(Me_4N)^+$ cations, crystals **3** and **4** prefer an antiparallel alignment (Figure 7b) of the $[Cd(XCN)_3^-]_\infty$ zigzag chains with the primitive crystal lattice in space group $Pna2_1$. This crucial structural difference has important implications in terms of the physical properties of these coordination solids, as we shall discuss next.

IV. Discussion

The ambidentate XCN^- ligand (X = S, Se, Te), with a hard N atom and a softer X atom as donor atoms, tends to form polymeric structures with transition metal ions such as Cd(II). For nonlinear optical responses,[24−27] as exemplified by the 1-D cadmium−chalcogenocyanate $[Cd(XCN)_3^-]_\infty$ system of the title compounds, the asymmetric ligand arrangement and hence the highly asymmetric electronic distribution around the cadmium atoms are automatically realized by the trans influence, with the X atoms (X = S, Se) being trans to the N atoms, around the octahedrally coordinated Cd(II) atom (see Figure 5 for X = Se). However, it has been found[5−8] that the crystal structures of the IPOS series are, to a large extent, influenced by the cations. In other words, the cations serve not only as spacers, filling in the voids between the chains, but also as controllers, dictating the alignment of the $[Cd(XCN)_3^-]_\infty$ zigzag chains. For instance, as predicted previously by us,[5−8] the tetrahedrally coordinated tetraalkylammonium cations in the title compounds (Et_4N^+ in **1** and **2** and Me_4N^+ in **3** and **4**) should induce the formation of noncentrosymmetric space groups, making them potential candidates for such applications as second harmonics generation. However, while all four structures (**1**−**4**) adopt noncentrosymmetric space groups, only tetraethylammonium salts (**1** and **2**) give rise to SHG effects. This was, at first glance, a puzzle. A detailed analysis of these structures, however, revealed a fundamental difference in the alignment of the $[Cd(XCN)_3^-]_\infty$ zigzag chains (where X = S or Se) in the solid state. As shown in Table 2, in both compounds **1** and **2**, the $[Cd(XCN)_3^-]_\infty$ chains are aligned in a parallel fashion (Figure 7a) whereas in compounds **3** and **4**, the $[Cd(XCN)_3^-]_\infty$ chains are aligned in an antiparallel fashion (Figure 7b). We believe that the antiparallel alignment results in the cancellation of the dipole moments from individual chains, resulting in the nullification of the net dipole moment for the crystal and hence no second harmonic generation. On the other hand, for the parallel alignment, dipole moments from the individual chains add up to produce a net dipole moment for the crystal that is a prerequisite for the macroscopic SHG properties. We therefore conclude that for the 1-D system noncentrosymmetry must be augmented by parallel alignment of the chains, as exemplified by the $[Cd(XCN)_3^-]_\infty$ chains in **1** (X = S) and **2** (X = Se). In fact, in these structures, the parallel chain alignment is afforded by the crystallographic *C*-centering (with space group $Cmc2_1$).

In addition to the above-mentioned "structural control" of the SHG effect, another surprising result of the present study is the discovery that compound **2** is phase-matched while compound **1** is not. According to the Kurtz−Perry analysis,[22] if the average particle size *d* is much smaller than the average coherence length l_c, it can be shown that for non-phase-matchable materials, the second harmonic generation should increase with increasing particle size. The situation for phase-matchable materials is more complex in this particle size regime. Nevertheless, arguments can be made that the SHG output should also increase with increasing particle size. In the case where the particle size *d* is much greater than the coherence length ($d \gg l_c$), the behaviors of the non-phase-matchable and phase-matchable materials are distinctly different. For non-phase-matchable materials, the total SHG intensity is inversely proportional to the particle size and goes to zero for very large particles. For phase-matchable materials, on the other hand, the

(24) Kanis, D. R.; Ratner, M. A.; Marks, T. J. *J. Am. Chem. Soc.* **1992**, *114*, 10338.

(25) (a) *Nonlinear Optical Properties of Organic and Polymeric Materials*; Williams, D. J., Ed.; ACS Symposium Series 23; American Chemical Society: Washington, DC, 1983. (b) *Materials for Nonlinear Optics: Chemical Perspectives*; Marder, S. R., Sohn, J. E., Stucky, G. D., Eds.; ACS Symposium Series 455; American Chemical Society: Washington, DC, 1991. (c) *Nonlinear Optical Properties of Organic Molecules and Crystals*; Chemla, D. S., Zyss, J., Eds.; Academic: Orlando, FL, 1987.

(26) Marder, S. R.; Kippelen, B.; Jen, A. K.-Y.; Peyghambarlan, N. *Nature* **1997**, *388*, 845.

(27) Verbiest, T.; Houbrechts, S.; Kauranen, M.; Clays, K.; Persoons, A. *J. Mater. Chem.* **1997**, *7*, 2175.

Table 3. Comparisons of Crystal Symmetry, Spatial Arrangement, and Relative Alignment of $[Cd(XCN)_3^-]_\infty$ Zigzag Chains (Where X = S for **1** and **3**, X = Se for **2** and **4**) and NLO Properties for Compounds **1**−**4**

compd formula	space group	spatial arrangement of $[Cd(XCN)_3^-]_\infty$ chains	alignment of $[Cd(XCN)_3^-]_\infty$ chains	SHG effect	phase-matchable (1.06 μm laser)
$[Et_4N][Cd(SCN)_3]$ (**1**)	$Cmc2_1$	hexagonal	parallel	yes	no
$[Et_4N][Cd(SeCN)_3]$ (**2**)	$Cmc2_1$	hexagonal	parallel	yes	yes
$[Me_4N][Cd(SCN)_3]$ (**3**)	$Pna2_1$	hexagonal	antiparallel	no	
$[Me_4N][Cd(SeCN)_3]$ (**4**)	$Pna2_1$	hexagonal	antiparallel	no	

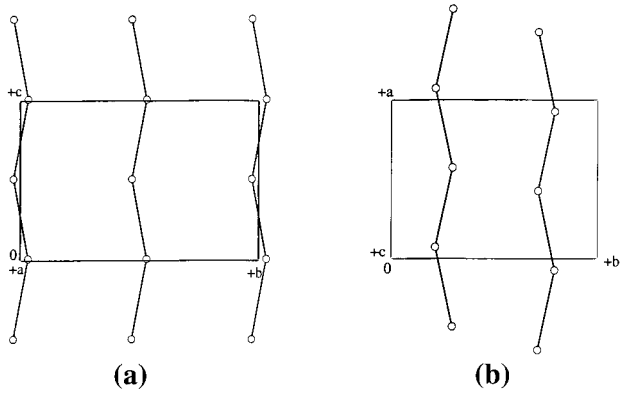

Figure 7. Cd atoms in $[R_4N^+][Cd(XCN)_3^-]$ where R = Et, X = S (**1**), Se (**2**); R = Me, X = S (**3**), Se (**4**) form infinite zigzag chains with Cd···Cd distances of 5.41 Å and Cd···Cd···Cd angles of 162° and with (a) parallel alignment in **1** and **2** and (b) antiparallel alignment in **3** and **4**.

observed second harmonic intensity is independent of particle size in this regime. Since coherence lengths are typically about 10−20 μm, large particle sizes generally imply >100 μm and small particle sizes are roughly a few micrometers. It can be seen from Figure 3 that **1** is not phase-matchable because the observed SHG intensity decreases with increasing particle size beyond about 50−60 μm. Compound **2**, on the other hand, is phase-matchable (see Figure 4) because the output of SHG signals increases with increasing particle size and reaches a plateau at about 50−60 μm.

V. Conclusion

In summary, the title compounds reported in this paper represent a series of highly promising hybrid (inorganic, organic, and polymeric) materials with tailorable molecular and crystal structures. It resembles the traditional inorganic and organic nonlinear optical (NLO) materials in some aspects but differs in many others. The beneficial properties or characteristics of this class of NLO crystals are as follows.[5−8] First, the anionic $[Cd(XCN)_3^-]_\infty$ chains (where X = S, Se, Te) form isolated (well separated) polymeric structures of low dimensionality (e.g., 1-D or 2-D), giving rise to anisotropic physical properties. Second, the extended π-conjugation system within the polymeric cadmium−chalcogenocyanate, with the high polarizabilities of both the metal and the ligand, gives rise to desirable physical properties such as NLO effects. Third, the cation serves as spacer/controller of the crystal structure and crystal symmetry. For nonlinear optical effects such as second harmonic generation, it is important to arrange the chains in a parallel fashion. Antiparallel alignment of the chains will effectively nullify any second-order NLO effect, even if the crystal structure adopts a noncentrosymmetric space group. Fourth, these coordination solids show typical properties of ionic compounds such as relatively high melting points and good mechanical properties. Fifth, the ability to fine-tune the molecular parameters (e.g., from S to Se to Te and from (Me_4N^+) to (Et_4N^+)) and the crystal structures (e.g., from $Pna2_1$ to $Cmc2_1$ and from antiparallel to parallel alignments of the anionic chains) opens the door to tailorable crystals with desirable physical properties. Finally, and perhaps most importantly, the combination of d^{10} metal such as Cd(II) and XCN^- ligands (where X = chalcogenide series) has the added advantage of being optically transparent from near-ultraviolet (220 nm) to near-infrared (3300 nm) regions (a very wide and continuous optical window indeed), making it useful for a wide variety of frequency conversion applications. Work is in progress to grow large-sized single crystals of the title compounds as new frequency-doubling crystals as well as for other device applications.

Acknowledgment. The authors thank the personnel of CHEMSYS, Inc. for the elemental analyses and Dr. Tom Cooper and his group for their generous technical support. Acknowledgment is also made to National Research Council to H.Z. (WPAFB) and National Science Foundation to B.K.T. (UIC) for financial support of this research.

Supporting Information Available: One X-ray crystallographic file, in CIF format, and two powder measurement data (Tables S1 and S2). This material is available free of charge via the Internet at http://pubs.acs.org.

IC9912833